

# Passing the Baton: High Throughput Distributed Disk-Based Vector Search with BatANN

Nam Anh Dang  
Cornell University  
Ithaca, New York  
nd433@cornell.edu

Ben Landrum  
Cornell Tech  
New York, New York  
blandrum@cs.cornell.edu

Ken Birman  
Cornell University  
Ithaca, New York  
ken@cs.cornell.edu

## ABSTRACT

Vector search underpins modern information-retrieval systems, including retrieval-augmented generation (RAG) pipelines and search engines over unstructured text and images. As datasets scale to billions of vectors, disk-based vector search has emerged as a practical solution. However, looking to the future, we need to anticipate datasets too large for any single server. We present BatANN, a distributed disk-based approximate nearest neighbor (ANN) system that retains the logarithmic search efficiency of a single global graph while achieving near-linear throughput scaling in the number of servers. Our core innovation is that when accessing a neighborhood which is stored on another machine, we send the full state of the query to the other machine to continue executing there for improved locality. On 100M- and 1B-point datasets at 0.95 recall using 10 servers, BatANN achieves **6.21–6.49×** and **2.5–5.10×** the throughput of the scatter-gather baseline, respectively, while maintaining mean latency below **6 ms**. Moreover, we get these results on standard TCP. To our knowledge, BatANN is the first open-source distributed disk-based vector search system to operate over a single global graph.

### PVLDB Reference Format:

Nam Anh Dang, Ben Landrum, and Ken Birman. Passing the Baton: High Throughput Distributed Disk-Based Vector Search with BatANN. PVLDB, 14(1): XXX-XXX, 2020.  
doi:XX.XX/XXX.XX

### PVLDB Artifact Availability:

The source code, data, and/or other artifacts have been made available at [https://github.com/namanhboi/rdma\\_anns](https://github.com/namanhboi/rdma_anns).

## 1 INTRODUCTION

In recent years, improvements in representation learning and the rise of retrieval augmented generation (RAG) [22] as a technique to improve accuracy and reduce hallucinations in LLM outputs has driven a surge in interest in vector search. Typically, an embedding model is used to encode unstructured data, such as a chunk of a document [1, 15] or an image [25] as a high dimensional vector. After a collection of items have been encoded this way, the same model or one trained jointly with the embedding model can be used to represent queries in such a way that among the embeddings,

This work is licensed under the Creative Commons BY-NC-ND 4.0 International License. Visit <https://creativecommons.org/licenses/by-nc-nd/4.0/> to view a copy of this license. For any use beyond those covered by this license, obtain permission by emailing info@vldb.org. Copyright is held by the owner/author(s). Publication rights licensed to the VLDB Endowment.

Proceedings of the VLDB Endowment, Vol. 14, No. 1 ISSN 2150-8097.  
doi:XX.XX/XXX.XX

the nearest neighbors of a query vector correspond to items in the dataset relevant to that query.

The embedding process itself is inexact, hence finding the exact nearest neighbors of a query vector is neither practical nor necessary (known data structures for exact nearest neighbor search have query complexity which is either linear in the number of vectors or exponential in the dimensionality of the vectors [6]). Instead, we use approximate nearest neighbor (ANN) search, finding a large fraction of the embeddings nearest to a query.

Because web-scale data sets can include billions of embeddings which are collectively too large to keep in memory, research into efficient disk-based search methods has been active. Today’s state-of-the-art methods, such as DiskANN[18] and Starling[32] rely on search graphs, an index type that supports empirically logarithmic query time with respect to dataset size [18, 36]. Considerable research has focused on optimizing the performance of these graph structures. However, the throughput of a single server running a disk-based system is bottlenecked by the bandwidth of SSDs attached to a single machine. This motivates *distributed disk-based search*, which allows the system to serve more queries per second (QPS) by leveraging multiple machines in parallel. This is the context for the present paper, which starts by assuming that a large data set has been sharded (partitioned) across a cluster of compute nodes.

There are two natural ways to distribute a graph-based index. The first is to partition the dataset into disjoint subsets and build a graph index independently for each [7, 12, 31]. At query time, the system searches all partitions and merges their results. The second is to construct a single global graph over the entire dataset and then partition the nodes of the graph—i.e., its neighbor lists and embeddings—across multiple servers.

Because the first method does not fully exploit the sub-linear scaling of search graphs, recent work has pushed toward scalable distributed traversal of a global ANN graph. For example, CoTra [38] offers an in-memory distributed vector search system that leverages RDMA networking. DistributedANN [1] proposes a disk-based distributed system built on commodity networking hardware. These systems differ in how they orchestrate inter-server communication during search, but both generally rely on a request-reply pattern to explore off-server neighbors during traversal.

We present BatANN<sup>1</sup>, a new approach for distributed disk-based vector search over a global graph that achieves high throughput and low latency with standard TCP networking. The core innovation of our system is its asynchronous, state-passing query procedure, which forwards entire query states between servers. This design

<sup>1</sup>Pronounced “baton”, a reference to the relay-like behavior of the query procedure.

maximizes data locality and avoids the round-trip communication overhead found in current distributed global graph approaches.

We make the following contributions:

- We propose a new distributed search mechanism for disk-based vector search that achieves near linear scaling in throughput in high recall regimes even on TCP.
- We show that our system has minimal latency penalty when scaling up the number of servers and sustains its low latency even at very high query rates.
- We open source our implementation and evaluate its performance against best available baselines in distributed disk based search on various 100M and 1B scale datasets.

## 2 BACKGROUND

Formally,  $k$  nearest neighbor ( $k$ -NN) search is defined as follows. Given a set of vectors  $X \subset \mathbb{R}^d$ , a distance function  $\delta : (\mathbb{R}^d \times \mathbb{R}^d) \rightarrow \mathbb{R}$  and a query vector  $q \in \mathbb{R}^d$ , find a set  $\mathcal{K} \subseteq X$  such that  $|\mathcal{K}| = k$ , and  $\max_{p \in \mathcal{K}} \delta(p, q) \leq \min_{p \in X \setminus \mathcal{K}} \delta(p, q)$ . We use ‘point’ and ‘vector’ interchangeably to refer to elements of  $X$ . There exist other notions of nearest neighbor search (most notably  $\epsilon$ -NN), but we focus exclusively on  $k$ -NN as it’s the dominant paradigm in the literature and practical application. Unless otherwise mentioned,  $\delta$  is squared euclidean distance for the purposes of this work.

Graphs have been studied as a method of indexing vectors for nearest neighbor search since the late 1990s [4], although they have more recently become the dominant paradigm for scalable, low-latency vector search [10, 18, 36]. In a *search graph*, each vector in the dataset being indexed corresponds to a node in a graph. The edges are chosen in such a way that greedy traversal of the graph yields near neighbors of a query vector: starting from some node in the graph and comparing the query to its neighbors, the neighbor nearest the query is chosen as the next node to expand. In naive greedy search, this process is repeated until a point is reached which does not have any neighbors closer to the query than itself. Our goal is to find  $k$  neighbors, hence the classical greedy search is replaced with *beam search*, where a *beam* consisting of the best  $L$  points seen so far is recorded, and at each step, the best point in the beam which has not yet had its neighbors expanded is explored. This repeats until the beam converges to a set of points that all have been explored. Pseudocode for the beam search algorithm is presented in algorithm 1.

Practical vector search systems often combine indexing with *quantization*: methods that store a lossy representation of the vectors in the dataset to enable approximate distance comparisons with a much smaller footprint. For systems requiring high accuracy, some number of results larger than  $k$  are retrieved using the quantized vectors, and *reranked* using exact distance comparisons computed with the original vectors, with the  $k$  nearest neighbors returned being the true nearest neighbors within the group selected with the quantized vectors.

The most popular quantization scheme is product quantization (PQ) [21]. PQ is used in our system for almost all distance comparisons. To encode a set of vectors, PQ first splits each vector into subspaces which each consist of a slice of the dimensions of the vector space. Then, given a parameter  $b$  representing the number of bits to store per subspace,  $k$ -means clustering with  $k = 2^b$  is done

---

### Algorithm 1: Beam Search

---

```

Input:  $G$  = graph,  $q$  = query vector,  $W$  = I/O pipeline width
Output:  $k$  nearest vectors to  $q$ 
1  $s \leftarrow$  starting vector;
2  $L \leftarrow$  candidate pool length;
3 candidate pool  $P \leftarrow \{\langle s \rangle\}$ , explored pool  $E \leftarrow \emptyset$ ;
4 while  $P \not\subseteq E$  do
5    $V \leftarrow$  top- $W$  nearest vectors to  $q$  in  $P$ , not in  $E$ ;
6   Read  $V$  from memory or disk;
7    $E$ .insert( $V$ );
8   for  $nbr$  in  $V$ .neighbors do
9      $P$ .insert( $\langle nbr, \delta(nbr, q) \rangle$ );
10   $P \leftarrow L$  nearest vectors to  $q$  in  $P$ ;
11 return  $k$  nearest vectors to  $q$ ;

```

---

to find a set of cluster centroids for each subspace, which are stored along with the quantized vectors. The compressed representation of each vector is then the cluster assignments of each of its subspaces, which for feasible values of  $b$  is considerably smaller than the original float-valued vector. At query time, a vector can be reconstructed by concatenating the centroids to which it was assigned, and distances can be computed with respect to the reconstructed vector. Optimized implementations favor constructing a *codebook* consisting of precomputed distances between each centroid and the corresponding subspace for a query [3, 20]. Distances can then be computed by summing the contributions of the centroids to which a point has been assigned.

The accuracy of ANN search is measured in terms of *recall*, which is the average fraction of points in an output of length  $k$  which are at least as close to the query as the true  $k$ -th nearest neighbor.

### 2.1 Disk-based vector search

The problem of scaling fast and accurate vector search to dataset sizes beyond what can fit in DRAM on a single node has been an active area of research for several years. Our work builds on DiskANN, which was the first SSD-optimized solution able to index billions of vectors while preserving performance competitive with an in-memory index [18]. The index is designed around a paradigm in which in-memory PQ data is used to guide beam search to select the best  $W$  candidate nodes in the beam to explore and read its full embedding and neighbor ID list from disk. All  $W$  SSD reads are then issued in parallel. DiskANN additionally introduces what is called a Vamana [18] search-graph construction, which seeks to minimize the number of hops in the graph needed for search to converge, and proposes an efficient algorithm for constructing such a graph over the points in the dataset. Data within the graph is clustered so that each point’s unquantized vector and its neighborhood will fit within a 4KB disk sector. During beam-search, a highly compressed PQ representation of the dataset is kept in memory and used to decide which nodes to search next.

Additional prior work is reviewed in Section 7.

### 3 DISTRIBUTED VECTOR SEARCH

Our work is best understood in the context of other implementations of distributed disk-based vector search. These broadly fall into two categories, which we now review.

#### 3.1 Scatter–Gather Approaches

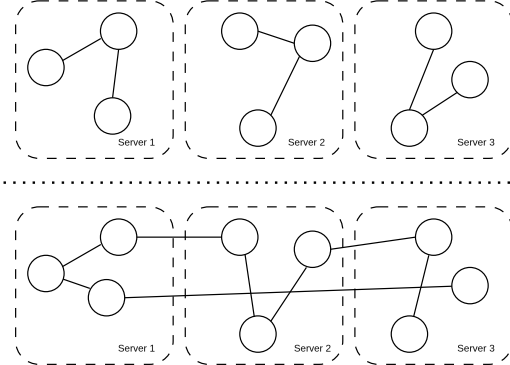


Figure 1: Scatter–Gather vs. Global Index

Many distributed vector search systems employ some variant of a scatter–gather paradigm. As seen in Figure 1, these approaches split the dataset into shards which can be distributed to discrete nodes, and build indexing data structures on the points in each shard independently. At query time, a query vector is distributed to some or all of the shards (the “scatter”), and each independently queries its local index for near neighbors. The results are then collected and merged (the “gather and reduce” step) into an approximation of the global near neighbors of the query. Commercial vector databases using this approach such as [9, 31] are further discussed in subsection 7.2.

#### 3.2 Distributed Global Indices

In contrast to the scatter–gather approach, DistributedANN [1] and CoTra [38] build a global graph index over the full dataset, distribute it across several machines, and run queries on the global index using sophisticated data-dependent communication patterns which are meant to leverage the highly data-dependent behavior of queries on a graph index<sup>2</sup>. Provided that sufficient work can be done locally, the advantage of this global graph is its improved query complexity: queries on search graphs are roughly logarithmic in the size of the dataset, and the sum of the logarithms of sizes of shards will always be larger than the logarithm of the sum [38]. This is the same broad approach used by our system. Because both systems are most relevant to our system, we choose to explain them more in-depth below:

**DistributedANN** [1] is meant to emulate DiskANN [18] while running in a distributed setting, using a distributed KV store in place of the local SSD in DiskANN. Query routing is handled by a centralized orchestration layer, which receives queries and uses an in-memory routing index to initialize search in the same way as

<sup>2</sup>Note that at the time of writing, neither CoTra nor DistributedANN is publicly available. As a result, we will not be able to use either as a baseline against which our work could be compared.

Starling[32]. After search on the routing graph converges, each step of the traversal involves the orchestration layer querying nodes which store the neighborhoods of the graph and vectors in the dataset, using the returned results to update the beam and decide which nodes to query in the next step.

Notice that *each step of beam search requires a round trip between the orchestrator and one or more servers with relevant vectors*. Our work departs from DistributedANN in viewing these round-trips as problematic in servers that need to run at the highest possible query rates: each time an orchestrator thread pauses to collect results, resources are locked up on the orchestrator, and because the number of concurrent orchestrator threads running in a node is limited, we could reach a state in which nodes are underutilized because their orchestrator threads are all waiting.

**CoTra** [38] is an in-memory distributed search system that builds a global graph which is distributed across nodes networked with remote direct memory access hardware: RDMA. At query time, a central routing index identifies ‘primary’ shards which contain a large number of relevant points, and ‘secondary’ shards which are expected to be less relevant. Each primary node then maintains its own beam, and issues asynchronous requests and remote reads to other primary and secondary partitions to get neighborhoods and distance comparisons. The beams of the primary nodes are regularly synced in a procedure called co-search.

A concern raised by CoTra is the cost of the RDMA hardware on which it depends. Even as MLs are becoming more and more dependent on RAG databases, security and privacy issues are forcing more and more of them to operate in dedicated servers on the premises of the data owners. RDMA may simply price these users out of a CoTra-like solution.

Notice that both the above approaches rely on a send/receive pattern of communication where some query state on one server is dependent on distance computation results or one-sided RDMA reads of data held in the memories of other servers. In the next section, we discuss the BatANN architecture, which introduces a new asynchronous flow communication pattern in which entire queries are handed off from server to server as computation progresses. The focus shifts: in BatANN, our goal will be to do as much work as we can at each hop of the task.

### 4 THE BatANN APPROACH

As discussed in [38], a single global index brings the benefit that query times are logarithmic in the size of the search graph. It is not evident that this would still be true for a distributed collection of individually indexed and queried partitions. Indeed, a problematic trend is evident in the experiments we will present in Section 6: with existing scatter–gather approaches, the number of distance comparisons and disk I/O rises proportionally with the number of servers involved.

Our problem can thus be stated as follows: *Given a global graph, what is the most efficient way to distribute and query a search graph across many nodes without introducing unacceptably high latency from communication?* As we have seen, one direction focuses on relatively costly hardware, such as RDMA [38] or CXL [17] networking. There has been some work aimed at leveraging low-latency disaggregated memory technologies, but these remain somewhat

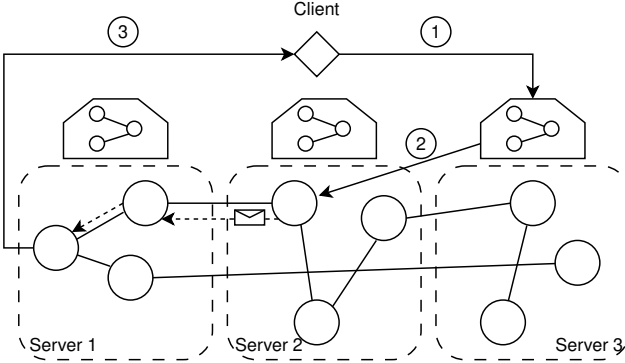


Figure 2: System overview

exotic today. We target a more common case, where nodes are connected by commodity networking hardware and communicate using TCP, but in doing so must embrace the sweet spot for this protocol, which can sustain very high throughput but is not ideal for round-trip interactions. Accordingly, our design prioritizes reducing the amount of time queries spend waiting on communication, in much the same way that single-node disk-based indices minimize the number of round trips to disk.

To this end, we first construct a graph over the entire dataset and partition it across servers using a technique from Gottesburen et.al [12], ensuring that consecutive traversal steps are likely to access nodes stored on the same machine. A query is then dispatched to one of these servers to first conduct search on an in-memory head index to get the starting nodes of a beam-search execution (① and ② in Figure 2). During beam-search execution, when an off-server computation is required—i.e., when all current best candidate nodes reside on a remote server—we avoid the overhead of request-response round-trips by **sending the full query state** directly to the destination server (Envelope in Figure 2). This distributed beam search then executes until all nodes in the beam are explored, at which point the server holding the state sends the result back to the client (③ in Figure 2).

In this new and highly asynchronous paradigm, the latency penalty from communication is cut in half relative to requesting data from another machine and waiting for a response; as soon as the query state reaches the other server, it can take over execution using local data. Latency is also reduced with the help of neighborhood-aware graph partitioning. A partition/server will advance a query state for as many steps as possible until it has to transfer this state to another server.

By sending the entire state of the beam search execution for a query, our approach avoids performing additional distance computations compared to DiskANN on a single server for  $W = 1$ . For higher  $W$ , by using algorithm 2 to adapt the I/O pipeline to a distributed graph, we are also able to hold the number of distance comparisons done by BatANN to be approximately the same as for a single instance of DiskANN.

#### 4.1 What is a State?

We can see from Algorithm 1 that beam search progresses step-by-step. In disk-based search, each step takes the  $W$  closest frontier nodes in the beam—sorted by their approximate distances to the query—and issues disk reads for their full embeddings and neighbor IDs. Using the retrieved embeddings, we compute full-precision distances to the query, which will later be used for the final reranking stage. We then mark these  $W$  nodes as explored and attempt to insert their neighbors into the beam based on in-memory PQ distances while maintaining a maximum beam size of  $L$ . The search concludes when all nodes in the beam have been explored, at which point we rerank the beam using the full-precision distances accumulated throughout the search to obtain the final  $k$  results.

To advance a beam-search execution, the system must carry the beam state, and the full-precision result list, along with the parameters  $L$ ,  $k$ , and  $W$ . For large beam sizes ( $L \geq 200$ ), which are often necessary to achieve recall above 0.95, the total state size—including the query embedding—is approximately 4-8 KB. Transferring several kilobytes of state across machines for every inter-partition hop is non-trivial when using TCP. Consequently, minimizing the frequency of inter-server state transfers becomes critical for both throughput and latency. This motivates the next two components of the system: the in-memory head index and the global graph partitioning.

#### 4.2 In-Memory Head Index

From Zhang et. al [37], we know that a given run of beam search can generally be divided into two distinct phases. During the first phase, the algorithm approaches the general neighborhood of the query, and during the second phase, beam search stabilizes near the neighborhood of the query. This means that the beam explores many portions of the graph before settling into a region near the query. Since we are partitioning the graph across multiple servers, the first phase is likely to involve inter-server communication. Similar to CoTra and DistributedANN, we employ an in-memory head-index built from a 1% sample of the graph to determine the starting nodes of beam-search. This head-index is replicated across all servers (① Figure 2).

More sophisticated approaches exist for this initial routing stage, such as building a KD-tree during index construction to guide routing at query time [34]. We choose the 1% sampling method for its simplicity and demonstrated effectiveness in prior disk-based vector search systems [1, 32], but with the assumption that the decision might need to be revisited. This has not been necessary.

#### 4.3 Graph Partitioning

To reduce the number of times a state has to be sent between servers, we can partition the graph so that nearby points are likely to reside on the same server. As this is analogous to the property of search graphs that makes neighbors likely to be connected by an edge, spatial partitioning algorithms like balanced  $k$ -means [2] can be used to put neighbors of a point on the same server, thereby leveraging compute-data locality. Balanced  $k$ -means is what CoTra [38] uses to partition its global graph across servers. We use a partitioning algorithm based on one proposed by Gottesburen et. al [12], which is faster to run and is known to out-perform balanced  $k$ -means in the

scatter-gather approach. Our intuition is that the algorithm is more effective in preserving spatial relationships between graph nodes, yielding better locality and reduced inter-server communication.

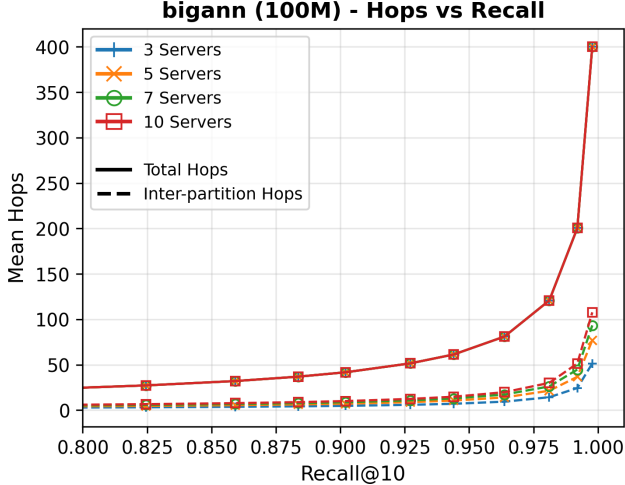


**Figure 3: Number of hops vs. inter-partition hops for BIGANN 100M on 3, 5, 7, 10 servers with  $W = 1$ . Inter-partition hops only account for 11.6-24.3% of total hops, validating the choice to use graph partitioning.**

To isolate the effect of graph partitioning, we will explore the number of inter-partition hops for best first search, a variant of beam search in which  $W = 1$ . With best-first search, at any given step, the beam will only choose to explore the best unexplored candidate node.

From Figure 3, we observe that at 0.95 recall@10, inter-partition hops account for 11.6%, 17.34%, 21.22% and 24.3% of total hops in the 3-, 5-, 7- and 10-server configurations, respectively. Because each inter-partition hop incurs communication and serialization overhead, these proportions translate directly to latency. We also see that the total number of hops is identical regardless of the number of servers used, which is expected for best-first search because both systems index the same global graph. The low frequency of inter-partition hops validates our graph partitioning approach.

#### 4.4 I/O Pipeline Width

In this subsection, we explore the effects of higher I/O pipeline width  $W$  on our system’s performance and justify the usage of  $W = 8$ , which has minimal impact on the number of distance comparisons and disk reads while decreasing the number of inter-partition hops.

DiskANN shows that increasing the I/O pipeline width  $W$  can reduce search latency. Modern consumer-grade SSDs can sustain more than 300K random reads per second, so issuing  $W$  reads concurrently incurs roughly the same latency as issuing a single read [18]. By processing multiple items in the beam at once, the I/O pipeline also decreases the total number of beam-search hops. However, larger values of  $W$  necessarily introduce some computational waste: many of the vectors and neighbor lists retrieved at higher

pipeline widths are not close enough to the query to be inserted into the beam, even though their embeddings were read and neighbor distances were computed. DiskANN found that  $W \in \{2, 4, 8\}$  strikes a good balance between latency and throughput, and this is consistent with our observations.

In a distributed global graph, strictly following the standard beam-search procedure is not possible because some nodes selected for the I/O pipeline may reside on remote servers’ SSDs. To support the I/O pipeline in this setting, we introduce a simple heuristic described in algorithm 2.

---

**Algorithm 2: Heuristic for I/O Pipeline in Distributed Global Graph**

---

**Input:** beam  $P$ , pipeline width  $W$   
**Output:** next action for beam search

- 1  $V :=$  top  $W$  unexplored nodes of  $P$
- 2 **if**  $V$  has nodes on current server **then**
- 3   **explore** all nodes on current server in  $V$
- 4 **else**
- 5   **send state to the server containing the top node in  $V$ ;**

---

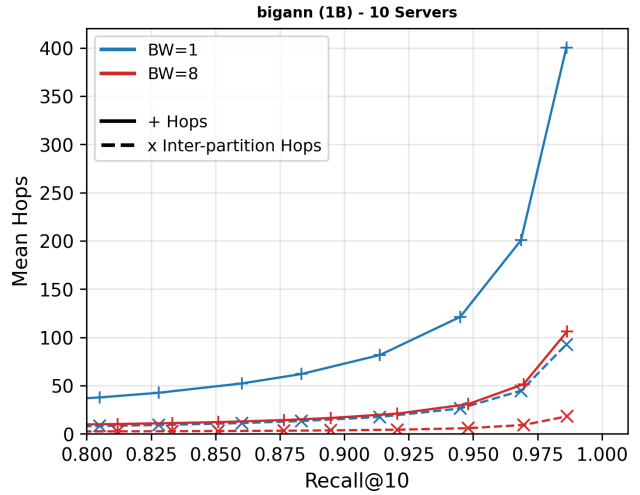


**Figure 4: Comparison of inter-partition hops between  $W = 1, 8$  for BIGANN 1B on 10 servers. Higher  $W$ , fewer total and inter-partition hops.**

This heuristic serves two purposes. First, when all pipeline nodes are local, we benefit from the same latency improvements provided by the I/O pipeline in single-server settings. Second, it enables the I/O pipeline to operate efficiently in a distributed setting for larger values of  $W$  by reducing the number of inter-partition hops, thereby lowering the overhead introduced by serialization and the network stack.

Figure 4 shows that the total hop count decreases by nearly a factor of four when increasing  $W$  from 1 to 8 at 0.95 recall@10. For  $W = 1$ , the mean hop count is 138.1, whereas for  $W = 8$  it is 32.6.

This follows naturally from the fact that processing more nodes per iteration reduces the number of beam-search rounds/hops. Inter-partition hops scale proportionally with the total hop count for both  $W$  values, accounting for 21.9% of hops at  $W = 1$  and 18.8% at  $W = 8$ .

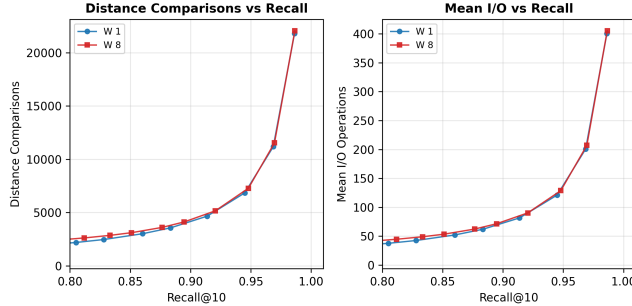


**Figure 5: Comparison of Distance Computations and Disk I/O issued between  $W = 1, 8$  for BIGANN 1B on 10 server. Both  $W$  values are nearly identical across all recall values.**

Additionally, as we can see in Figure 5, the number of distance computations and Disk I/O are almost the exact same for both  $W = 1, 8$  across all recall values. Distance computations and Disk I/O are the 2 main bottlenecks for disk-based vector search. Therefore,  $W = 8$  achieves better throughput and latency than  $W = 1$  since it reduces the number of inter partition hops while maintaining similar computation and I/O efficiency. We explore this improvement in more depth in subsection 6.6.

## 5 IMPLEMENTATION AND OPTIMIZATIONS

We implemented BatANN using C++ and base our single-server implementation on PipeANN’s publicly available codebase [13]. `io_uring` was used for asynchronous I/O, and inter-server communication was handled by the ZeroMQ library [29], specifically the PEER socket. We also used the `moodycamel::ConcurrentQueue` [8] concurrent queue throughout the system.

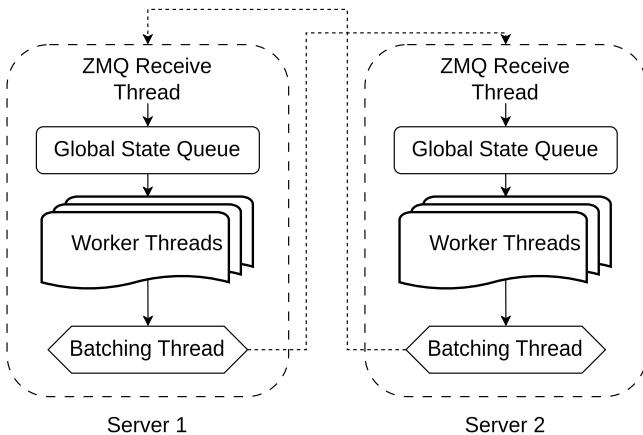


**Figure 6: System implementation**

The inner structure of a single BatANN process are shown in Figure 6. The system runs a dedicated ZeroMQ receiver thread responsible for listening on a bound address, receiving incoming objects, and deserializing them before placing them into the appropriate queues. One such object is a query state, which the receiver places into a global state queue for the worker threads to consume. To send states or results, worker threads enqueue them into an outgoing queue that the batching thread monitors. The batching thread then opportunistically batches messages and sends them to other servers or clients. Below we present some optimizations found during system implementation.

**Inter-query Balancing on a Single Thread:** In most prior work on disk-based vector search [18, 28, 32], each search thread executes one query at a time. As observed by [13], this is suboptimal: during greedy search, each step requires reading the neighbor IDs of a candidate node from disk, leaving the compute thread idle while waiting for disk I/O to complete. This naturally motivates balancing multiple queries per thread, allowing the system to overlap computation for one query with asynchronous disk I/O (e.g., via `io_uring`) for others. We build on PipeANN’s implementation of inter-query balancing [13]. Their inter-query balancing approach processes queries in batches: as queries in a batch complete, the number of active queries per thread temporarily decreases, and only returns to the full batch size once the next batch is submitted. In contrast, our system maintains a fixed number of active queries (or states) per thread at all times. When a query finishes, the thread immediately pulls the next query from the queue, ensuring that the number of queries being balanced is fixed. In our experiments, balancing 8 queries concurrently yielded the best overall performance. We discuss the performance of this fixed-size query balancing vs. other approaches in subsection 6.1.

**Caching Query Embedding:** Query embeddings are sent to each server only once. A server caches the embedding until it receives an acknowledgment from the client indicating that the final result has been delivered. This avoids repeatedly transmitting the same embedding alongside every state message. This optimization is also used in CoTra [38].

**Pre-allocating objects:** To eliminate allocation overhead during message deserialization, we use object pooling for all message types exchanged between servers (e.g., search states and query embeddings). When a communication handler thread receives an incoming message, it deserializes directly into a pre-allocated object obtained from a lock-free queue (`moodycamel::ConcurrentQueue` [8]). This removes dynamic allocation from the critical receive path and improves system throughput. After processing, worker threads then return the pre-allocated objects to their respective pools for reuse.

**Memory footprint:** We keep a PQ representation of the full dataset in memory on each node, with each vector compressed to 32 bytes. For 100M and 1B scale, this equates to 3.2 GBs and 32 GBs respectively. This PQ data is used to compute the approximate distances to neighbors of a node, whose IDs are fetched from disk. As discussed in [28], we can store relevant PQ data alongside neighbor IDs on disk with close to no penalty in throughput or latency, in exchange for an increase in the size of the index. We identify this as a promising extension for future work. Additionally, we keep the map of `node_ids` to partition ids, which is used to send the

state of the beam-search execution. The partition ids are stored as uint8, and for 100M and 1B scale, this accounts for 0.1 and 1GB respectively. For points residing on a given node, we also keep a mapping of node ids to disk sector ids to know where to read from. This type of mapping is used in disk-based methods where nodes are not stored contiguously by id on disk like [32]. At billion scale, this mapping doesn't exceed 1 GB.

## 6 EXPERIMENTS

**Setup:** We conduct all experiments on a CloudLab [11] cluster of 10 c6620 nodes connected by 25Gb-Ethernet. The c6620 nodes each have a 28-core Intel Xeon Gold 5512U at 2.1GHz and 128GB ECC Memory (8x 16 GB 5600MT/s RDIMMs) and runs Ubuntu 22.04 LTS.

**Datasets:** We evaluate our system using three publicly available datasets, BIGANN, DEEP, and MSSPACEV, from the Big-ANN benchmarks [26]. All datasets are evaluated at 100M scale, with BIGANN and MSSPACEV also evaluated at 1B scale. BIGANN contains 128-dim uint8 SIFT descriptors and serves as a classic large-scale ANN benchmark. MSSPACEV provides 100-dimensional int8 embeddings from Microsoft's SpaceV model for semantic search, representing a modern quantized workload. DEEP consists of 96-dimensional floating-point descriptors extracted from deep convolutional networks. Together, these datasets cover a diverse range of vector types and dimensionalities, enabling a broad evaluation of system performance. A summary is given in Table 1.

Table 1: Datasets used in the experiments

Dataset	Scale	Dim	Type	Similarity
BIGANN	1B/100M	128	uint8	L2
MSSPACEV	1B/100M	100	int8	L2
DEEP	100M	96	float	L2

**Graph Construction:** All of our indices at both the 100M and 1B scales are Vamana graphs [18] built with parameters  $R = 64$ ,  $L = 128$ , and  $\alpha = 1.2$ . For the 100M datasets, we constructed the indices using the PipeANN codebase. For the 1B datasets, we generated the graphs using ParlayANN [23] and then merged them with the corresponding datasets to produce the final disk-based indices. We do this because the ParlayANN graph construction is faster at billion scale.

**Graph partitioning:** We partitioned the dataset using the codebase from [12] and used their graph partitioning method. We use another server with 96 cores and 1.5 TB of DRAM to partition the billion scale dataset. This is because partitioning at billion scale using the method in [12] has peak memory usage of 1.25TB, 10x that of the memory available in the c6620 Cloudlab nodes.

**Baselines:** We compare our system against the scatter-gather approach described in Figure 3.1. Partitions are assigned using the same method as BatANN from [12]. Each server uses the inter-query balancing approach we described in section 5. The partitions use the same graph construction parameters as the full dataset, as experiments and precedent from prior work [23] suggest that parameter choice for Vamana graph construction is not sensitive to the size of the dataset being indexed. In our experiments, we call this baseline ScatterGather. As remarked earlier, DistributedANN does

not share an open source implementation, making it impossible to compare our approach directly (we actually tried to re-implement the DistributedANN approach, but our version did not achieve competitive throughput or latency relative to our system or the ScatterGather baseline). For the same reason, we exclude CoTra: the code base is not open and the system is deeply dependent upon RDMA.

**Metrics:** We measure throughput using plots of Queries-per-second (QPS) versus recall@10, a value typical for evaluations of systems for approximate nearest neighbor search [5].

### 6.1 Single Server

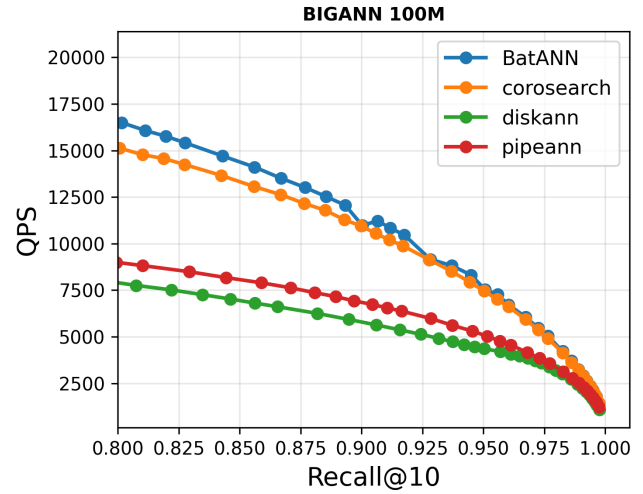


Figure 7: QPS recall graph of different search methods on BIGANN 100M with 8 threads.

We find that the inter-query balancing approach used in our system provides consistently higher throughput across recall regimes. For this reason, we adopt it both as our single-server baseline in scaling experiments and as the underlying search procedure for our implementation of scatter-gather. Figure 7 compares the throughput of our implementation against DiskANN, PipeANN, and CoroSearch, the inter-query balancing implementation provided in PipeANN.

To measure the QPS-recall curve of our approach, we issue queries from a separate client process, which introduces additional overhead from TCP communication and serialization. The other search methods issue queries directly in the same process, using OpenMP dynamic scheduling and directly invoke the search function, avoiding these costs. As a result, if DiskANN, PipeANN, and CoroSearch were re-implemented and evaluated under the same client/server setup as ours, their measured throughput would be slightly lower due to communication overhead.

### 6.2 Throughput

For all throughput experiments, we issue all the queries at once on the client side round robin order to the servers and wait for all the

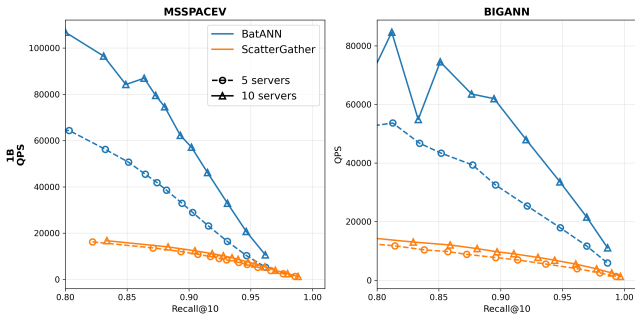


**Figure 8: QPS recall curve of BIGANN, MSSPACEV on 5 and 10 servers for 1B. BatANN outperforms ScatterGather on all setups**

results to come back before calculating QPS and recall. For both ScatterGather and BatANN, each server runs 8 search threads.

**Performance at 100M scale.** As can be seen in Figure 9, for 5 servers, BatANN achieves **2.93-3.98x** QPS improvement for 0.95 recall@10 across all datasets. For 10 servers, the improvement is even more dramatic. BatANN achieves **6.21-6.49x** QPS improvement for 0.95 recall@10 compared to the ScatterGather baseline. The biggest improvement, 6.49x the throughput of ScatterGather, is with the DEEP dataset. For both the 5 and 10 server setups, there is also broadly higher throughput than baselines across all recall regimes.

**Performance at 1B scale.** From Figure 8, we see that BatANN continues to substantially outperform ScatterGather across all recall regimes and server counts. For the BIGANN dataset, at recall@10 0.95, the throughput advantage is **3.70x** (5 servers) and **5.10x** (10 servers). The MSSPACEV dataset is more difficult for BatANN, with a 1.5x improvement in throughput at 5 servers and 2.5x improvement at 10 servers. This however, is not exactly an issue with the BatANN, but more an issue with the search graph performance for MSSPACEV at 1 Billion scale in general. We used ParlayANN to construct the 1B graph, and they observed similar drop in throughput at the 0.95 recall@10 region (Figure 3b in their paper [23]).

Having said that, these numbers show that the same trends observed at 100M scale persist at 1B: BatANN’s throughput gains grow with the number of servers, reflecting the efficiency advantage of the global graph approach compared to independent sharding for ScatterGather. This advantage is explored in subsection 6.3.

### 6.3 Computation and I/O Efficiency

To measure computational efficiency we record the total number of distance comparisons performed per query. We also recorded the number of disk IO operation issued. Jointly, these account for the vast majority of the runtime of a vector search query.

For ScatterGather, each server independently searches its own disjoint index, so the reported numbers are the sum of distance comparisons and disk I/O operations across all servers. Consequently, the total amount of computation and disk I/O performed by ScatterGather increases proportionally with the number of servers, as shown in Figure 10. In contrast, notice the clear efficiency advantage of BatANN. We attribute this advantage to the heuristic described

in algorithm 2, which effectively replicates the I/O pipeline behavior of an index on a single node in a distributed setting. Indeed, BatANN performs nearly the same number of distance comparisons and Disk I/O as on a single server in both the 5- and 10-server configurations. Because the amount of computation and I/O remains essentially constant across server counts, BatANN is able to achieve near-linear weak scaling, as discussed in subsection 6.4.

### 6.4 Scalability

From Figure 11, we see that BatANN benefits far more from strong scaling than the scatter-gather approach. Because distance comparisons and by extension a large part of the work of querying, remain the same for our approach regardless of the number of machines, throughput is able to improve as more cores become available. Additionally, the amount of Disk I/O is essentially the same compared to a single instance of DiskANN but is spread out across more servers. This means that BatANN is able to avoid the disk throughput bottleneck that hampers SingleServer throughput as we scale up the number of threads.

However, as BatANN partitions become smaller as the number of servers increases, it becomes less likely for consecutive steps to reside on the same node. This leads to more inter-partition hops—seen in Figure 3—which adds communication overhead. This is why we see mildly sub-linear scaling as the number of servers increases.

### 6.5 End-to-End Latency

We define end-to-end latency as the time between a client issuing a query and receiving the corresponding result. Prior single-server systems and evaluations [13, 18] typically issue queries within the same search process using OMP dynamic scheduling and measure latency as the duration of the search function call. This methodology does not translate cleanly to a distributed setting where queues necessarily have to be used.

Accordingly, we split up our experiments into 2 sections. First we compare end-to-end latency for BatANN and ScatterGather at a low send-rate—1000 QPS—to see how the systems perform with no queuing artifacts. Then look at how latency degrades (or doesn’t) when we issue sends at rates close to max throughput for 0.95 recall@10.

**6.5.1 1K Send Rate.** As shown in Figure 12, BatANN achieves **end-to-end latency below 5 ms** at 0.95 recall@10 on both the 5-server and 10-server clusters. Moreover, the latency on 10 servers is only 13% higher than on 5 servers.

From Figure 10, we observe that the amount of disk I/O—the dominant bottleneck for latency in disk-based vector search [13, 18]—remains nearly identical across both configurations. Figure 10 further shows that the number of distance comparisons is almost the exact same in both settings. These similarities arise from the fact that both configurations search over the same global graph and therefore perform essentially the same amount of work per query. It also highlights the effectiveness of algorithm 2 at adapting the I/O pipeline in a distributed setting. The only meaningful difference is the higher number of inter-partition hops in the 10-server setup. Each hop requires transmitting a search state to another server,

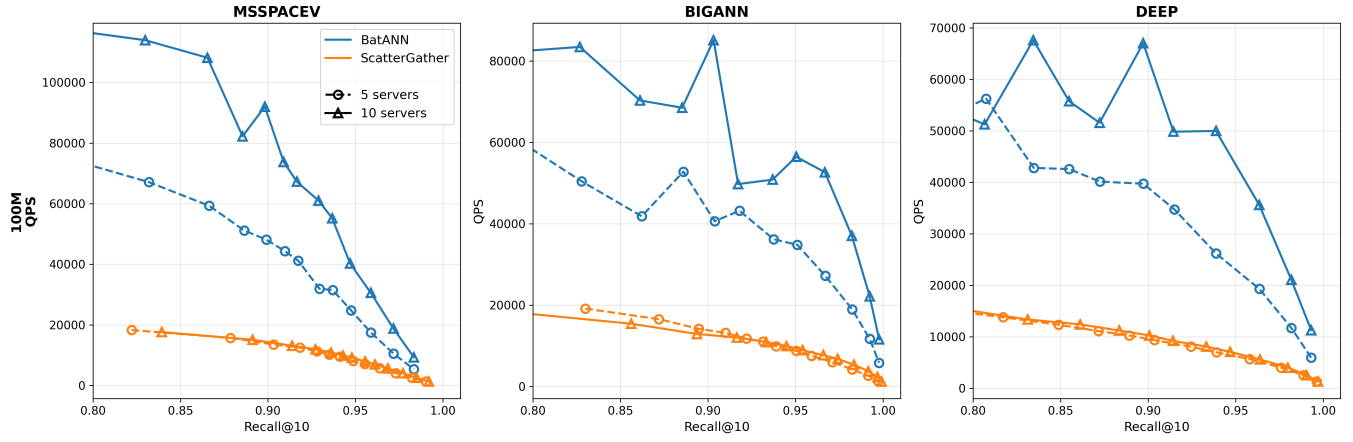


Figure 9: QPS recall curve of BIGANN, MSSPACEV, DEEP on 5 and 10 servers for 100M. BatANN outperforms ScatterGather on all setups

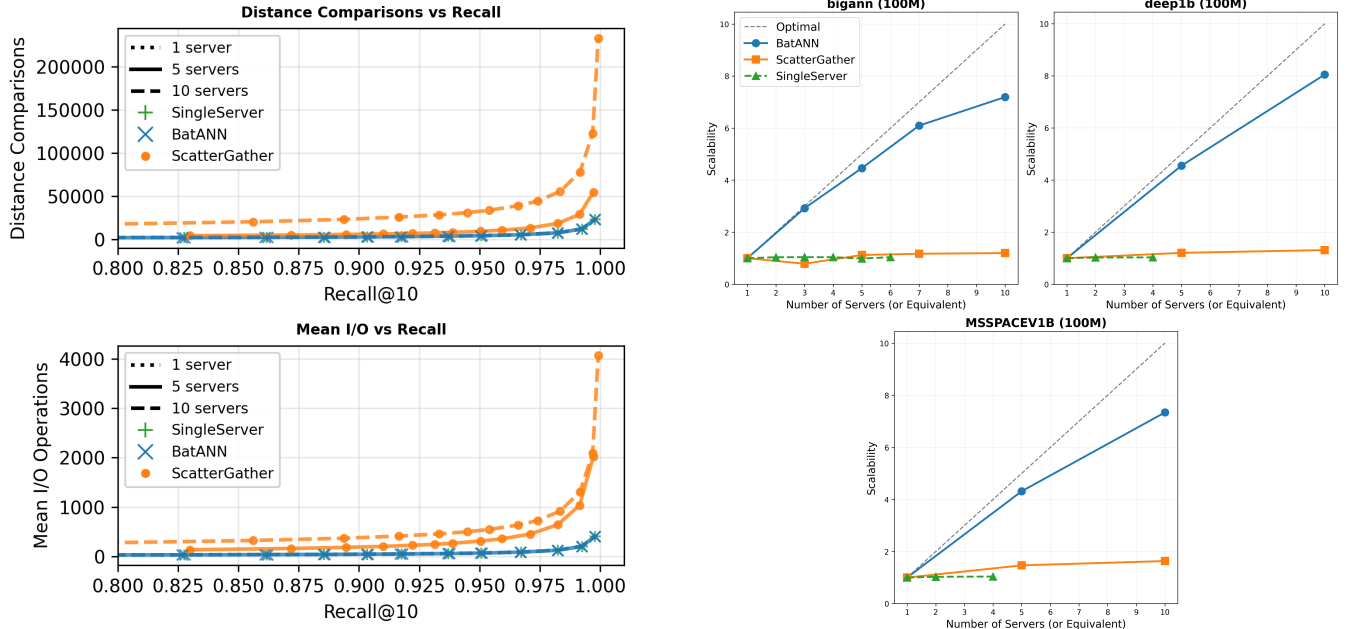


Figure 10: Distance comparisons and I/O vs. recall plot of BIGANN 100M on 5 and 10 server setups with  $W = 8$ . BatANN is clearly more computationally and I/O efficient, doing essentially the same amount of computation and Disk I/O as a single DiskANN instance.

which incurs serialization and network-stack overhead. This additional communication cost accounts for the modest increase in end-to-end latency.

ScatterGather latency is better than BatANN because its latency is only dependent on the slowest query for each of the disjoint partitions. These disjoint partitions are smaller than the global index, which makes it faster to query them. Also, ScatterGather

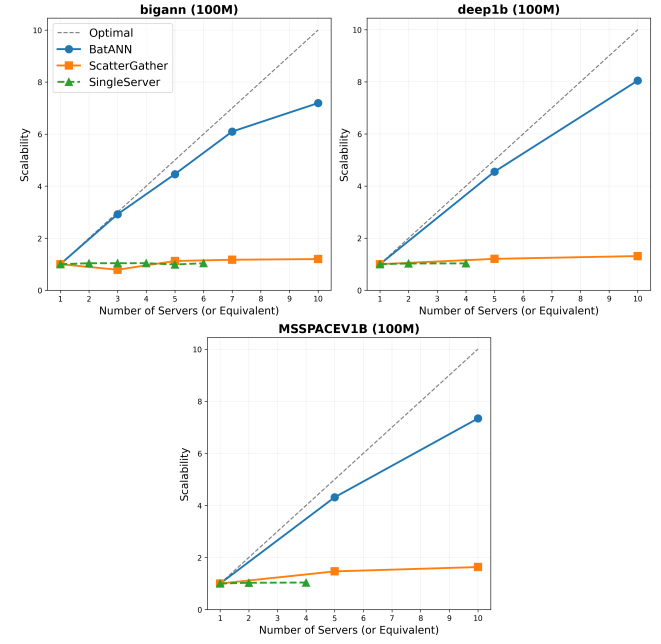
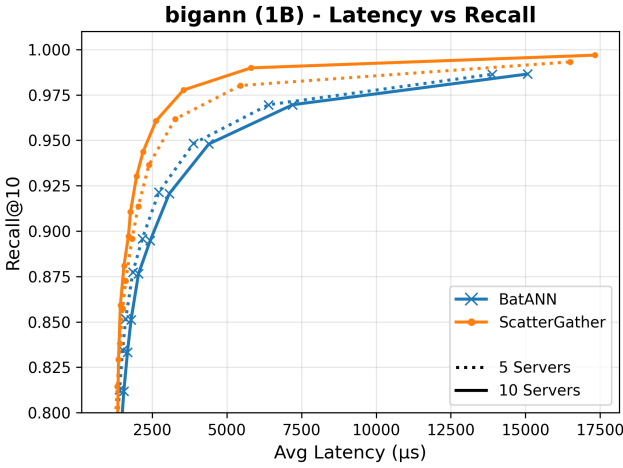


Figure 11: Scalability on BIGANN, MSSPACEV, DEEP at 100M up to 10 servers at  $W = 8$  and  $\text{recall}@10 = 0.95$ . SingleServer represents an 8-thread baseline scaled proportionally with the number of servers. BatANN achieves near-linear scaling.

latency is lower for the 10 server configuration than with 5 servers, which is to be expected since the size of the index is halved.

**6.5.2 Latency vs. Send Rate for 0.95 recall.** From Figure 8, we can see that at 0.95 recall@10, throughput for ScatterGather and BatANN are around 6000 and 30000 QPS respectively. Hence, we choose to examine how latency changes as we increase the send rate up to these thresholds. As we can see in Figure 13, as send rate increases from 1000 to 6000, ScatterGather's mean and tail latency



**Figure 12: Latency Recall curve of BIGANN 1B on 5, 10 server setup with  $W = 8$  at 1K send rate. Slight increase in BatANN latency when scaling up.**

rises accordingly. In contrast, BatANN’s mean latency only rises marginally as the send rate increases from 6000 to 10000 and stabilizes at around 6ms thereafter.

One thing to note is that BatANN’s latency spread is wider than ScatterGather, and its tail latency is worse. This is expected since BatANN is dependent on multiple hops of inter-server communication. The simple communication pattern used in ScatterGather reduces throughput but does benefit the per-query latency.

## 6.6 Beam Width Ablation

We see significant improvements in throughput and latency from the I/O pipeline optimization described in subsection 4.4. Looking at Figure 14, we can see that  $W = 8$  has broadly higher throughput at all recall regimes and less than half the latency of  $W = 1$  at 0.95 recall@10.

Both  $W = 1, 8$  require a similar amount of computation and issue similar numbers of disk reads. However, as we saw in Figure 4,  $W = 8$  has 4x fewer inter-partition hops than  $W = 1$ , which explains its superior efficiency in both throughput and latency. This fact coupled with the analysis in subsection 6.5 highlights that inter-partition hops are the main barrier to achieving linear scalability.

## 7 RELATED WORK

### 7.1 Disk-based vector search

PipeANN [13], is a disk-based graph index that achieves lower latency and higher throughput than DiskANN by relaxing the order of operations in beam search and by adjusting the size of the beam during search. Instead of issuing some number of parallel reads and waiting until all of them have returned to move on to the next step of search, PipeANN eagerly processes the results of pipelined reads as they return, issuing reads for the most promising neighbors of the fetched neighborhood, potentially before the results of slower reads from earlier steps of search have been received. Additionally, by realizing that beam-search has 2 distinct phases [37], they created a

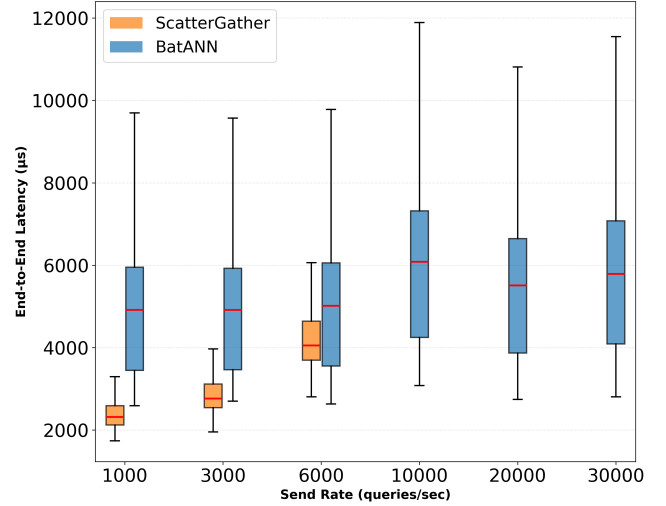


**Figure 13: Box and whisker plots of end-to-end latency for varying query send rates for BatANN and ScatterGather at 0.95 recall@10 on BIGANN 1B on 10 servers. Each method is run for QPS values up to the measured maximum throughput for that method, as higher send rates have tail latencies which are a function of the number of queries being run. ScatterGather performance collapses after 6000qps; BatANN is stable to 30000qps.**

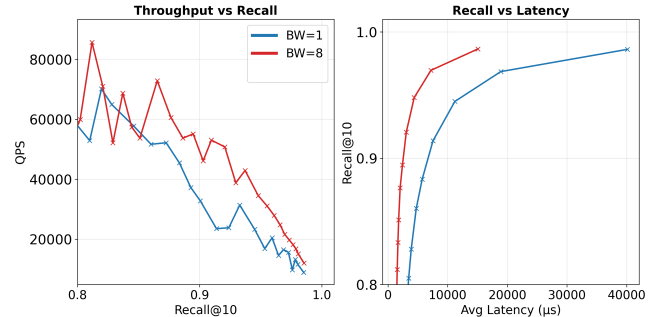


**Figure 14: Throughput and latency comparison for  $W = 1, 8$  for BIGANN 1B on 10 servers.  $W = 8$  has higher performance across regimes with respect to both metrics.**

heuristic to detect which phase the search is currently in and adjust the I/O pipeline accordingly.

Further optimizations for single-node DiskANN focus on reorganizing vector layout on disk. DiskANN stores vectors contiguously by ID, which provides no locality guarantees for graph neighbors. Starling [32] improves both throughput and latency by co-locating the neighbors of each node within the same disk sector, massively improving locality during beam-search. They also introduce a beam-search variant tailored to this layout.

The size of a single DiskANN index is constrained not only by SSD capacity but also by memory, because DiskANN stores the PQ representation of every vector in memory. Recent work, including

AiSAQ [28] and DistributedANN [1], attempt to circumvent this limitation by storing compressed vector representations alongside each node’s neighbor list on disk. AiSAQ observes that this approach produces essentially no degradation in latency or throughput. However, because neighbors appear in multiple adjacency lists, these compressed vectors are duplicated across the graph, substantially inflating the size of an already-large disk-resident structure [1].

## 7.2 Other Distributed Vector Search Systems

Our earlier discussion of related work in section 3 focused on approaches that resemble BatANN in the use of a global graph distributed across several machines. Here we describe other approaches that attempt to solve the same problem but in different ways.

**Vector Databases:** At least two popular vector database products describe using a scatter-gather approach to distributed search: Milvus [31, 32] and Pinecone [16]. In both, data is split into discrete shards (“segments” for Milvus and “slabs” for Pinecone), which are each individually indexed and stored. At query time, the results from querying each independently are combined to form a global result set.

**Cosmos DB [30]:** Cosmos DB, a popular distributed NoSQL database product from Azure, supports indexing vectors for ANN queries with DiskANN. Indices can be sharded, in which case a standard scatter-gather approach is used to perform queries.

**Pyramid [7]:** Pyramid describes a system which implements a series of optimizations over building HNSW [36] graphs over disjoint shards at each node. A global “meta-HNSW” index is used to identify the most relevant shards for each query, and results from querying those shards are aggregated to get the global result.

**SQUASH [24]:** SQUASH uses a serverless architecture for scalable distributed vector search. This approach has tradeoffs typical for a serverless application, and is not well suited to the high-throughput, low-latency regime we target.

## 8 DISCUSSION

Our work leaves open a number of topics for future investigation:

**Reducing Message Size:** In the current design, each state transfer includes both the beam and the full result set, where the latter is derived from the vector embeddings encountered so far. The size of the result set scales with the number of hops as  $\text{hops} \times (\text{sizeof}(\text{float}) + \text{sizeof}(\text{node\_id}))$ . For large values of  $L$  (e.g., 200–400), which are required to reach very high recall, this result set can reach up to 3.2 KB. However, the result set is only needed for the final reranking stage once beam search has concluded. Instead of sending it along with every state transfer, we can send the result data directly to the client whenever a server hands off a query state. The client can then aggregate all partial results and perform the final reranking locally, similar to the scatter-gather approach.

**Exploration of Other Disk-Based Optimizations:** As discussed above, PipeANN found considerable improvement in throughput and latency by relaxing the ordering in which to process nodes in I/O pipeline and by adjusting  $W$  mid-flight. Because BatANN leverages similar techniques for parallel reads, adapting their beam width adjustment to the unique characteristics of our system may

present opportunities to improve our latency and throughput. Additionally, it would be worthwhile to explore adapting the indices of Starling [32] to a distributed setting. Because Starling uses a variant of beam search tailored to their disk layout, BatANN would require a different heuristic than algorithm 2 to fully exploit this disk-based optimization.

**Distributed Global Graph Updates:** A wealth of prior work has studied ways to support in-place updates to search graphs without compromising the quality of the index or periodically re-indexing [14, 27, 33, 35]. The distributed nature of our system presents unique challenges in this area. After removing a point from the graph, in-neighbors of that point which may be spread across several nodes need to update their neighborhoods as not to route search to a point which no longer exists.

**Efficient Fault Tolerance:** Our current system is not robust to node failures. Our plan is to port BatANN to run on the sharded storage framework supported by Derecho [19], which has an efficient fault-tolerant replication solution. Derecho would also enable us to experiment with dynamic updates and to explore load-balancing options among shard members.

**Network Accelerators:** Previous work on global distributed graph indices has leveraged RDMA and CXL [17, 38], which require more specialized and expensive hardware than our TCP-based approach. Because our design is based on a high-speed asynchronous data-relaying scheme centered on query states that are only a few kilobytes in size (an object size at which datacenter TCP performs well), it is unclear that RDMA would really bring much benefit. However, because Derecho can be configured to use RDMA by changing a single parameter, porting to that library will make it easy to test this hypothesis.

**Multitenancy:** As RAG MLs expand in use, many enterprises will find it necessary to maintain multiple vector databases as a way to prevent leakage of data with restricted access permissions. Hosting multiple vector databases on a shared set of servers would open a wide range of scheduling and resource-sharing issues.

## 9 CONCLUSION

We present BatANN, a novel system for distributed disk-based ANNS. The core innovation of BatANN is that we query a global graph by sending query state between machines when beam search expands a node on another server. This allows us to achieve better latency, faster communication, and improved locality, while preserving the number of disk reads and distance comparisons compared to a single node baseline.

## ACKNOWLEDGMENTS

This work was supported by funds provided by Microsoft and IBM. We thank CloudLab and their supporters for access to machines. We also thank Alicia Yang for valuable input and technical support.

## REFERENCES

- [1] ADAMS, P., LI, M., ZHANG, S., TAN, L., CHEN, Q., LI, M., LI, Z., RISVIK, K. M., AND SIMHADRI, H. V. DistributedANN: Efficient Scaling of a Single DiskANN Graph Across Thousands of Computers. In *The 1st Workshop on Vector Databases* (July 2025).
- [2] AHALT, S. C., KRISHNAMURTHY, A. K., CHEN, P., AND MELTON, D. E. Competitive learning algorithms for vector quantization. *Neural Networks* 3, 3 (Jan. 1990), 277–290.

[3] ANDRÉ, F., KERMARREC, A.-M., AND SCOURNEC, N. L. Quicker ADC : Unlocking the hidden potential of Product Quantization with SIMD. *IEEE Transactions on Pattern Analysis and Machine Intelligence* 43, 5 (May 2021), 1666–1677.

[4] ARYA, S., AND MOUNT, D. M. Approximate nearest neighbor queries in fixed dimensions. In *Proceedings of the fourth annual ACM-SIAM symposium on discrete algorithms* (Austin, Texas, USA, 1993), Soda '93, Society for Industrial and Applied Mathematics, pp. 271–280. Number of pages: 10 tex.address: USA.

[5] AUMÜLLER, M., BERNHARDSSON, E., AND FAITHFULL, A. ANN-Benchmarks: A benchmarking tool for approximate nearest neighbor algorithms. *Information Systems* 87 (Jan. 2020), 101374.

[6] CHÁVEZ, E., NAVARRO, G., BAEZA-YATES, R., AND MARROQUIN, J. L. Searching in metric spaces. *Acta Computing Surveys* 33, 3 (Sept. 2001), 273–321.

[7] DENG, S., YAN, X., NG, K. K. W., JIANG, C., AND CHENG, J. Pyramid: A General Framework for Distributed Similarity Search, June 2019. arXiv:1906.10602 [cs].

[8] DESROCHERS, C. A Fast General Purpose Lock-Free Queue for C++. [moodycamel.com](http://moodycamel.com) (2014).

[9] DILOCKER, E., VAN LUIJT, B., VOORBACH, B., HASAN, M. S., RODRIGUEZ, A., KULAWIAK, D. A., ANTAS, M., AND DUCKWORTH, P. Weaviate, Nov. 2025. original-date: 2016-03-30T15:03:17Z.

[10] DONG, W., MOSES, C., AND LI, K. Efficient k-nearest neighbor graph construction for generic similarity measures. In *Proceedings of the 20th International Conference on World Wide Web* (2011), ACM, pp. 577–586.

[11] DUPLYAKIN, D., RICCI, R., MARICQ, A., WONG, G., DUERIG, J., EIDE, E., STOLLER, L., HIBLER, M., JOHNSON, D., WEBB, K., AKELLA, A., WANG, K., RICART, G., LANDWEBER, L., ELLIOTT, C., ZINK, M., AND CECCHET, E. The design and operation of CloudLab. In *Proceedings of the USENIX annual technical conference (ATC)* (July 2019), pp. 1–14.

[12] GOTTESBÜREN, L., DHULIPALA, L., JAYARAM, R., AND LACKI, J. Unleashing Graph Partitioning for Large-Scale Nearest Neighbor Search, Mar. 2024. arXiv:2403.01797.

[13] GUO, H., AND LU, Y. Achieving {Low-Latency} {Graph-Based} Vector Search via Aligning {Best-First} Search Algorithm with {SSD}. In *19th USENIX Symposium on Operating Systems Design and Implementation (OSDI 25)* (2025), pp. 171–186.

[14] GUO, H., AND LU, Y. OdinANN: Direct Insert for Consistently Stable Performance in Billion-Scale Graph-Based Vector Search. *24th USENIX Conference on File and Storage Technologies (FAST '26)* (2026).

[15] HUANG, P.-S., HE, X., GAO, J., DENG, L., ACERO, A., AND HECK, L. Learning deep structured semantic models for web search using clickthrough data. In *Proceedings of the 22nd ACM international conference on Information & Knowledge Management* (San Francisco California USA, Oct. 2013), ACM, pp. 2333–2338.

[16] INGBER, A., AND LIBERTY, E. Accurate and efficient metadata filtering in pinecone's serverless vector database. In *The 1st workshop on vector databases* (2025).

[17] JANG, J., CHOI, H., BAE, H., LEE, S., KWON, M., AND JUNG, M. CXL-ANNS: Software-Hardware collaborative memory disaggregation and computation for Billion-Scale approximate nearest neighbor search. In *2023 USENIX Annual Technical Conference (USENIX ATC 23)* (2023), USENIX Association, pp. 585–600.

[18] JAYARAM SUBRAMANYA, S., DEVVRIT, F., SIMHADRI, H. V., KRISHNASWAMY, R., AND KADEKODI, R. DiskANN: Fast Accurate Billion-point Nearest Neighbor Search on a Single Node. In *Advances in Neural Information Processing Systems* (2019), vol. 32, Curran Associates, Inc.

[19] JHA, S., BEHRENS, J., GKOUNTOUVAS, T., MILANO, M., SONG, W., TREMEL, E., RE-NESSE, R. V., ZINK, S., AND BIRMAN, K. P. Derecho: Fast state machine replication for cloud services. *ACM Trans. Comput. Syst.* 36, 2 (Apr. 2019).

[20] JOHNSON, J., DOUZE, M., AND JÉGOU, H. Billion-Scale Similarity Search with GPUs. *IEEE Transactions on Big Data* 7, 3 (July 2021), 535–547.

[21] JÉGOU, H., DOUZE, M., AND SCHMID, C. Product Quantization for Nearest Neighbor Search. *IEEE Transactions on Pattern Analysis and Machine Intelligence* 33, 1 (Jan. 2011), 117–128.

[22] LEWIS, P., PEREZ, E., PIKTUS, A., PETRONI, F., KARPUSHIN, V., GOYAL, N., KÜTTLER, H., LEWIS, M., YIH, W.-T., ROCKTÄSCHEL, T., RIEDEL, S., AND KIELA, D. Retrieval-augmented generation for knowledge-intensive NLP tasks. In *Advances in neural information processing systems* (2020), H. Larochelle, M. Ranzato, R. Hadsell, M. Balcan, and H. Lin, Eds., vol. 33, Curran Associates, Inc., pp. 9459–9474.

[23] MANOHAL, M. D., SHEN, Z., BLELLOCH, G., DHULIPALA, L., GU, Y., SIMHADRI, H. V., AND SUN, Y. ParlayANN: Scalable and deterministic parallel graph-based approximate nearest neighbor search algorithms. In *Proceedings of the 29th ACM SIGPLAN Annual Symposium on Principles and Practice of Parallel Programming* (New York, NY, USA, 2024), PPoPP '24, Association for Computing Machinery, pp. 270–285.

[24] OAKLEY, J., AND FERHATOSMANOGLU, H. SQUASH: Serverless and Distributed Quantization-based Attributed Vector Similarity Search, Feb. 2025. arXiv:2502.01528 [cs].

[25] RADFORD, A., KIM, J. W., HALLACY, C., RAMESH, A., GOH, G., AGARWAL, S., SASTRY, G., ASKELL, A., MISHKIN, P., CLARK, J., KRUEGER, G., AND SUTSKEVER, I. Learning Transferable Visual Models From Natural Language Supervision. In *Proceedings of the 38th International Conference on Machine Learning* (July 2021), PMLR, pp. 8748–8763. ISSN: 2640-3498.

[26] SIMHADRI, H. V., AUMÜLLER, M., INGBER, A., DOUZE, M., WILLIAMS, G., MANOHAL, M. D., BARANCHUK, D., LIBERTY, E., LIU, F., LANDRUM, B., KARJKAR, M., DHULIPALA, L., CHEN, M., CHEN, Y., MA, R., ZHANG, K., CAI, Y., SHI, J., CHEN, Y., ZHENG, W., WAN, Z., YIN, J., AND HUANG, B. Results of the big ANN: NeurIPS'23 competition, 2024. arXiv: 2409.17424 [cs.IR].

[27] SINGH, A., SUBRAMANYA, S. J., KRISHNASWAMY, R., AND SIMHADRI, H. V. FreshDiskANN: A Fast and Accurate Graph-Based ANN Index for Streaming Similarity Search, May 2021. arXiv:2105.09613 [cs].

[28] TATSUNO, K., MIYASHITA, D., IKEDA, T., ISHIYAMA, K., SUMIYOSHI, K., AND DEGUCHI, J. AiSAQ: All-in-Storage ANNs with Product Quantization for DRAM-free Information Retrieval, Feb. 2025. arXiv:2404.06004 [cs].

[29] THE ZEROMQ COMMUNITY. ZeroMQ: The intelligent transport layer, 2025.

[30] UPRETI, N., SIMHADRI, H. V., SUNDAR, H. S., SUNDARAM, K., BOSHIR, S., PERUMAL-SWAMY, B., ATRI, S., CHISHOLM, M., SINGH, R. R., YANG, G., HASS, T., DUDHEY, N., PATTIPAKA, S., HILDEBRAND, M., MANOHAL, M., MOFFITT, J., XU, H., DATHA, N., GUPTA, S., KRISHNASWAMY, R., GUPTA, P., SAHU, A., VARADA, H., BARTHWAHL, S., MOR, R., CODELLA, J., COOPER, S., PILCH, K., MORENO, S., KATARIA, A., KULKARNI, S., DESHPANDE, N., SAGARE, A., BILLA, D., FU, Z., AND VISHAL, V. Cost-Effective, Low Latency Vector Search with Azure Cosmos DB. *Proc. VLDB Endow.* 18, 12 (Aug. 2025), 5166–5183.

[31] WANG, J., YI, X., GUO, R., JIN, H., XU, P., LI, S., WANG, X., GUO, X., LI, C., XU, X., YU, K., YUAN, Y., ZOU, Y., LONG, J., CAI, Y., LI, Z., ZHANG, Z., MO, Y., GU, J., JIANG, R., WEI, Y., AND XIE, C. Milvus: A Purpose-Built Vector Data Management System. In *Proceedings of the 2021 International Conference on Management of Data* (Virtual Event China, June 2021), ACM, pp. 2614–2627.

[32] WANG, M., XU, W., YI, X., WU, S., PENG, Z., KE, X., GAO, Y., XU, X., GUO, R., AND XIE, C. Starling: An I/O-Efficient Disk-Resident Graph Index Framework for High-Dimensional Vector Similarity Search on Data Segment. *Proceedings of the ACM on Management of Data* 2, 1 (Mar. 2024), 1–27. arXiv:2401.02116 [cs].

[33] XU, H., MANOHAL, M. D., BERNSTEIN, P. A., CHANDRAMOULI, B., WEN, R., AND SIMHADRI, H. V. In-place updates of a graph index for streaming approximate nearest neighbor search. *CoRR abs/2502.13826* (Feb. 2025).

[34] XU, X., WANG, M., WANG, Y., AND MA, D. Two-stage routing with optimized guided search and greedy algorithm on proximity graph. *Knowledge-Based Systems* 229 (2021), 107305.

[35] XU, Y., LIANG, H., LI, J., XU, S., CHEN, Q., ZHANG, Q., LI, C., YANG, Z., YANG, F., YANG, Y., AND OTHERS. SPFresh: Incremental in-place update for billion-scale vector search. In *Proceedings of the 29th symposium on operating systems principles* (2023), pp. 545–561.

[36] YU, A. MALKOV, YU. A. MALKOV, YU. A. MALKOV, Y. A. D. A. YASHUNIN, AND YASHUNIN, D. A. Efficient and Robust Approximate Nearest Neighbor Search Using Hierarchical Navigable Small World Graphs. *IEEE Transactions on Pattern Analysis and Machine Intelligence* 42, 4 (Apr. 2020), 824–836.

[37] ZHANG, Q., XU, S., CHEN, Q., SUI, G., XIE, J., CAI, Z., CHEN, Y., HE, Y., YANG, Y., YANG, F., YANG, M., AND ZHOU, L. VBASE: Unifying online vector similarity search and relational queries via relaxed monotonicity. In *17th USENIX Symposium on Operating Systems Design and Implementation (OSDI 23)* (Boston, MA, July 2023), USENIX Association, pp. 377–395.

[38] ZHI, X., CHEN, M., YAN, X., LU, B., LI, H., ZHANG, Q., CHEN, Q., AND CHENG, J. Towards Efficient and Scalable Distributed Vector Search with RDMA, July 2025. arXiv:2507.06653 [cs].